# Investigation on Deformation of DP600 Steel Sheets in Electric-pulse Triggered Energetic Materials Forming

**Xueyun Xie**
harbin institute of technology
**HaiPing Yu** ( haipingy@hit.edu.cn )
harbin institute of technology
**Yang Zhong**
harbin institute of technology

**Research Article**

**Keywords:** High-velocity forming, Energetic materials, Pulse discharge characteristics, Numerical simulation, Plastic strain energy

**Posted Date:** December 15th, 2021

**DOI:** https://doi.org/10.21203/rs.3.rs-1148981/v1



**Version of Record:** A version of this preprint was published at The International Journal of Advanced Manufacturing Technology on March 11th, 2022. See the published version at https://doi.org/10.1007/s00170-022-09040-3.

# Abstract

Electric-pulse triggered energetic materials forming (ETEF) is a high-speed manufacturing process, which utilizes the chemical energy released by energetic materials (EMs) triggered by underwater wire discharge to plastically shape metals. The understanding of ETEF is not comprehensive, especially in the research on the discharge characteristics of energetic materials triggered by metal wires and the deformation process of metal sheets. In this paper, the above two problems were studied by means of experiment and numerical simulation. For the pulse discharge characteristics, the peak values of voltage and current were reduced during the triggering process of energetic materials. The triggering energy consumption of energetic materials was quantified to be about 200J. The matching parameters of different capacitor-voltage devices had no effect on triggering the energy release of energetic materials, so the electric pulse generator only played a triggering role on energetic materials. Compared with the quasi-static specimen with the same bulging height, the maximum major strain and thinning rate of the bulged specimen under ETEF condition were significantly reduced, and the deformation uniformity and strain distribution of the specimen were improved. The simulation results showed that the addition of energetic materials significantly improved the plastic strain energy of the blank. The deformation of the blank in ETEF can be divided into two stages: the initial chemical energy action stage and the inertia action stage. The bulging height of sheet metal increased by nearly 301% in inertia action stage, accounting for 80% of the total deformation time, and the effective plastic strain distribution was more uniform.


# 1. Introduction

To improve the fuel efficiency and crashworthiness of automobiles, the use of high strength steel to develop lighter and safer cars has become a trend in the automobile industry. Advanced high-strength steel sheets have been widely used in the production of impact-resistant and energy-absorbing components. However, the application of advanced high strength steel in auto-body components is still limited to simply shape automobile parts because it has difficulties in conventional deep drawing processes for complicated auto parts due to its poor formability. To further improve its strength and formability, it is necessary to select suitable forming process. Compared with traditional forming processes, high-rate forming (such as electromagnetic forming and electrohydraulic forming) is very effective in improving the strength and formability of materials, so many researchers have conducted research. At high strain rates, the flow stress of many materials increases significantly with the increase of strain rate [1–4], showing strain rate sensitivity. According to Psyk et al. [5], the workpiece is accelerated to a velocity of up to several hundred m/s and strain rates of $10^3$/s in the EMF process, thereby improving the formability and strength of the material, which will help enhance the crashworthiness of automotive parts.

Electromagnetic forming is a method that uses Lorentz force generated by pulsed magnetic field to deform workpiece at high speed [6–7]. Therefore, this non-contact feature of electromagnetic forming can significantly improve the surface morphology of the workpiece [8]. However, in practical applications, the forming capability of EMF is typically limited by the insulation strength and mechanical strength of the coil and the energy storage of the electric pulse generator. Increasing discharge energy will increase Lorentz force, but it will lead to insulation breakdown and coil breakage, which will affect the forming results and even damage the experimental equipment. Electrohydraulic forming is a high-rate forming technology in which shock waves generated by the discharge of two electrodes in a liquid medium cause plastic deformation of the workpiece [9]. Electrohydraulic forming uses water as a "punch" to form workpieces, so it exhibits high process flexibility. Additionally, because it

is not limited by the conductivity of materials, electrohydraulic forming is more widely used than electromagnetic forming. For instance, Golovashchenko et al. [10] and Tang et al. [11] successfully applied electrohydraulic forming to trimming of advanced high strength steel. Mamutov et al. [12] used electrohydraulic forming to manufacture a complex geometry automotive part. However, the energy utilization efficiency is extremely low due to the underwater electrode discharge, and even if the wire between the two electrodes is discharged, its energy utilization efficiency is only 24%, as concluded by Efimov et al. [13]. Therefore, this will cause a waste of energy.

Based on the above problems, Yu et al. [14] proposed a new high-velocity forming method, namely ETEF, which uses underwater metal wire electric explosion to ignite the chemical energy released by energetic materials to complete the deformation of the workpiece. It was found that energetic materials showed high energy effect, and the energy level of energetic materials was quantified as 3.04kJ/g through experiments. The discharge characteristics of underwater wire electric explosion have been studied by researchers. Han et al. [15] studied the underwater electrical explosion of copper wires and found that the deposited energy influenced the expansion of the discharge plasma channel and affected the shock wave characteristics. Grinenko et al. [16] conducted an experimental study on the underwater electric explosion of copper wire, and found that the efficiency of electrical energy deposition into the mechanical energy for the fluid flow was 25%, and the maximum pressure obtained at the boundary of discharge plasma channel was about 600MPa. However, the research on the discharge characteristics of energetic materials triggered by metal wires and the energy release level of energetic materials under different capacitance-voltage matching parameters is not clear, and the deformation process of workpieces in ETEF is not perfect. Therefore, it is necessary to conduct a comprehensive study of the above contents.

A better understanding of the discharge characteristics of energetic materials triggered by metal wires and the dynamic deformation process of the sheets in ETEF would help to implement this forming process in the automobile industry. Hence, in this work, the discharge characteristics of energetic materials triggered by metal wires under different capacitance-voltage matching parameters and the influence of energy release level of energetic materials on sheet bulging were evaluated. The deformation process of DP600 steel sheet in ETEF was studied by means of experiment and numerical analysis, such as strain distribution characteristics, deformation uniformity and dynamic deformation process.

# 2. Experimental Procedures

2.1. Materials description

The as-received material was cold-rolled DP600 steel sheet with a thickness of 0.8 mm, and provided by Baoshan Iron & Steel, co. China. The quasi-static tensile mechanical properties and main chemical compositions (wt.%) of this material are listed in Table 1.

**Table 1** Mechanical properties and chemical composition of the DP600 steel sheets.

| Yield Strength /MPa | Tensile Strength /MPa | Total elongation (engineering strain, %) | Uniform elongation (engineering strain, %) | Chemical composition wt (%) | | | | | | |
|---|---|---|---|---|---|---|---|---|---|---|
| | | | | Mn | Si | Ni | Cr | Cu | Al | Fe |
| 384.6 | 658.7 | 26.63 | 16.33 | 1.75 | 0.02 | 0.11 | 0.28 | 0.57 | 1.41 | 95.83 |

The new energetic materials selected in this study were aluminum (Al) particles and ammonium perchlorate (AP) particles. Al is a smooth sphere with an average particle size of 1–3 μm, and agglomeration occurs because of the small size of Al. AP particles showed irregular spheres with an average particle size of 140 μm. The energetic materials selected in this experiment—Al/AP (10 wt.% Al, 90 wt.% AP)—was prepared by physical mixing.

### 2.2. Energy release during ETEF

The electrical explosion of metal wires refers to the process of instantaneous melting and vaporization of metal wires to form plasma under high-voltage pulsed current. Plasma is heated and expanded by intense Joule heating and develops into a plasma channel filled with high pressure and high heat. During plasma diffusion, strong shock waves are radiated, which are quickly converted into sound pressure pulses and then spread to the surrounding medium, as described by Timoshkin et al. [17]. The ETEF method used the electric explosion of metal wire to form plasma, thus igniting energetic materials and releasing energy in water. The energy release process of energetic materials triggered by plasma can be divided into three stages: heating, ignition, and detonation (Fig. 1).

I. Heating stage: Under heat conduction of high temperature plasma, the temperature of solid energetic materials is rapidly heated from the initial temperature $T_0$ to the decomposition temperature $T_d$. No chemical reaction occurs during the process.

II. Ignition stage: Plasma continues to diffuse, causing the temperature of energetic materials to rise continuously from $T_d$ to $T_S$ (the burning surface temperature) and ignite. At this stage, energetic materials undergo a phase transition from solid to liquid and then to vapor and then produce high-temperature and high-pressure gas products on the surface.

III. Detonation stage: As energetic materials around the metal wire ignite, the gas temperature in stage II rapidly increases from $T_S$ to flame temperature $T_f$, and more energetic materials are ignited to release energy. Energetic materials decompose rapidly within a brief period to produce more gases. These gases expand quickly within a limited space, evolve into shock waves, and compress surrounding media to complete detonation.

Energetic materials react chemically and release high energy after ignition, described as heat and shock waves by Pagoria et al. [18]. Heat and shock waves locally heat up inside energetic materials to form "hot spots", leading to the rapid energy release of the entire energetic materials [19]. Energetic materials are characterized by high energy, a wide pulse, and a strong shock wave during energy release. Thus, they are widely used for infrared pulse radiation, exploitation of fossil energy, and rocket propulsion.

### 2.3. Experimental set-up for free bulging tests

Free bulging tests were carried out to investigate the deformation of DP600 steel sheet (with a diameter of 220mm) under a biaxial stress state. The schematic of experimental setups for bulging tests are illustrated in Fig. 2. In ETEF process, DP600 steel sheet was deformed by discharging metal wire with electric pulse generator, instantly igniting energetic materials, releasing chemical energy and generating shock wave in liquid chamber (Fig. 2(a)). The current and voltage generated by electric pulse generator discharging the metal wire were measured by the Rogowski current waveform transducer (Power Electronic Measurements Ltd, Nottingham, UK) and the P6015A high voltage probe (Tektronix, USA), respectively. Energetic materials were filled in EMs cylinder

with a length of 40mm. The top die was an open with an inner diameter of 100 mm and an entry radius of 10 mm. Fig. 2(b) shows the displacement variation with time during the sheet bulging process measured by position sensitive detector (PSD), namely a Laser Sensor M70LL (MEL Mikroelektronik GmbH, Germany). As shown in Fig. 2(c), in quasi-static free (QSF) bulging process, the dimension of punch was 100 mm in diameter and the fillet radius of the bottom die opening was 10mm.

An Optical three-dimensional (3D) deformation measuring system ARGUS-V6.3.1 (GOM GmbH, Germany) was used to obtain the plastic strain distribution of the deformed specimen. First, circular array grids with a diameter of 1 mm and an adjacent center distance of 2 mm were etched on the surface of the initial specimens by an electrochemical etching. Then, the strains data of the deformed grids were calculated by a GOM system.

2.4. Capacitance-voltage matching parameter tests

The Energetic materials in ETEF are triggered by plasma generated by wire explosion to release energy. Therefore, the influence of capacitance-voltage matching parameters in different electric pulse generators (EPG) on the variation characteristics of current and voltage after discharge and the energy release of energetic materials need to be studied in detail. Table 2 lists the discharge parameters of the two electric pulse generators and the quality of ignited energetic materials. The relationship between discharge energy $E$, equipment capacitance $C_i$ and discharge voltage $U$ can be expressed as:

$$E = 1/2\, C_i \cdot U^2 \qquad (1)$$

At the same discharge energy (1.37kJ), the discharge test of the same energetic materials (2g) triggered by different electric pulse generators were carried out. The effect of equipment parameters on the current and voltage waveform changes after the underwater discharge of pure metal wire and the discharge of energetic materials triggered by metal wire were studied. The waveform data of current and voltage were obtained by Rogowski current waveform transducer and Tektronix p6015a high voltage probe respectively, and the waveform results were displayed by an oscilloscope (Fig. 2(a)).

To study the influence of capacitance-voltage matching parameters on energy release of energetic materials in different electric pulse generators, we conducted discharge tests on energetic materials through two kinds of equipment parameters, and evaluated the influence of capacitance-voltage matching parameters on energy release of energetic materials through the final bulging height, deformation speed and effective plastic strain of the specimens during ETEF. The acquisition parameters were set as follows: displacement range, 0-50mm; sensitivity reached 0.4V/mm; acquisition frequency, 500 KHZ. The effective plastic strain of the deformed specimens was measured by the ARGUS-V6.3.1 testing system.

**Table 2** The discharge parameters of the two electric pulse generators and the quality of ignited energetic materials.

| Electric pulse generator | Rated capacitance, $C_i$ (μF) | Discharge energy, E (kJ) | Discharge voltage, U (kV) | EMs (g) |
|---|---|---|---|---|
| EPG-A | 304 | 1.37 | 3.0 | 2.0g |
| EPG-B | 100 | 1.37 | 5.23 | 2.0g |

# 3. Results And Discussion

3.1. Influence of capacitance-voltage matching parameters on discharge characteristics

The effect of capacitance-voltage matching parameters on the discharge characteristics of metal wires and its triggering energetic materials is the key link to study the energy release of energetic materials during ETEF process. Under the conditions of two equipment parameters (EPG-A, EPG-B), a metal wire (molybdenum wire with a diameter of 0.2mm and a length of 45 mm) and an EMs cylinder were used as the discharge object, and the discharge voltage *U(t)* and current *I(t)* were obtained, as shown in Fig. 3(a-b). According to Eqs. (2) and (3), the waveforms of instantaneous power $P_t$ and the deposited energy $W_t$ were calculated respectively (Fig. 3(c-d)).

$$P_t = I(t) \cdot U(t) \quad (2)$$

$$W_t = \int_0^t I(t) \cdot U(t)dt \quad (3)$$

According to the current and voltage curves presented in Fig. 3(a-b), at the same electrical pulse generator parameters, the addition of energetic materials resulted in a decrease in the maximum voltage of the wire before breakdown, and the peak value of current waveform decreased significantly after breakdown discharge. Generally, wire explosion will undergo a series of physical changes, that is, the phase transition from solid, liquid, gas to plasma. After the energetic materials were added, the physical process changed, and the plasma formed by wire explosion heated and ignited energetic materials for chemical reaction. In this process, the ignition of energetic materials occurred at the peak of voltage, which reduced the peak of current compared with the Mo wire explosion in water, indicating that the electrical conductivity changed during the ignition of energetic materials by metal wires. There are two reasons that may cause this phenomenon, one is that energetic materials are ignited, the other is that after wire explosion forms plasma, the nearby energetic materials are heated by thermal radiation to form a conductive layer, and the extra conductive layer (gas products produced by vaporization of energetic materials) increases the resistance of the discharge channel [20]. Both of these reasons can reduce the conductivity between electrodes and reduce the current in the circuit. Moreover, based on Eqs (2) and (3), calculated that the introduction of energetic materials reduced the maximum electric power and the electric energy deposited in the discharge channel. This phenomenon may be due to the fact that some energetic materials with high temperature are used as extra conductive substances, which accelerates the breakdown process of the wire vaporization discharge channel, resulting in a decrease in deposition energy. According to Fig. 3(c-d), it can be found that the energy consumed during the ignition of energetic materials was about 200J, so it can be inferred that energetic materials were ignited during the wire explosion, followed by chemical reactions and shock waves. Although energetic materials consumed the energy of plasma in the ignition process, the addition of energetic materials provided an additional shock wave amplitude, namely the secondary shock wave peak effect, which increased the impulse of the whole system, as demonstrated by Zhou et al. [21]. According to our previous studies [14], compared with pure electrohydraulic forming (discharge voltage 3kV), the bulging height of sheet metal under ETEF condition (3 kV/2 g) increased by 162%, so the shock wave energy produced by energetic materials is the fundamental reason for the significant increase of bulging height of sheet metal.

3.2. Influence of capacitance-voltage matching parameters on sheet bulging

In this section, the influence of energy release from energetic materials triggered by metal wire on sheet bulging is discussed under the matching parameters of capacitance-voltage of electric pulse generator. Fig. 4 presents the changing process of bulging height and deformation speed of sheet metal with time under different equipment parameters. It can be seen that the specimen was rapidly deformed in a short time, and the final bulging height was about 34mm. Under the conditions of two kinds of equipment, the speed of the apex (point A) of the bulged specimen changed with time as follows: the speed of the sheet reached the maximum at about 20μs, then dropped rapidly, and then rose slightly to maintain high speed movement, and the deformation speed was close to zero at about 300μs, finally until the end of deformation. Therefore, under different capacitance-voltage matching equipment parameters, the apex velocity of bulged sheet has the same trend with time in ETEF process. Additionally, according to our previous research [14], the variation trend of the peak velocity of the specimen obtained in ETEF numerical simulation under the parameter of 3 kV/2.0 g was in good agreement with the experimental results (Fig. 4(a)). Fig. 5 shows the bulged specimen and effective plastic strain under different equipment parameters. In the deformation zone of φ100mm, the distribution trend of effective plastic strain of the sheets under EPG-A and EPG-B equipment was similar, and the maximum effective plastic strain values were 49.3% and 50.4%, respectively. Table 3 lists the final bulging height, maximum deformation speed and maximum effective plastic strain obtained on the sheet under two kinds of equipment parameters, and their values are at the same level.

**Table 3** Deformation results of sheets in ETEF under different equipment parameters.

| Electric pulse generator | ETEF | Height, $H$(mm) | Max velocity, V (m/s) | Effective plastic strain, (%) |
|---|---|---|---|---|
| EPG-A | 3.0kV+2.0g | 34.0 | 255 | 49.3 |
| EPG-B | 5.23kV+2.0g | 34.5 | 252 | 50.4 |

According to the deposition energy curves in Section 3.1 (Fig. 3(c-d)), the deposition energy consumed by the ignition of energetic materials by metal wires was about 200J under different capacitance and voltage matching parameters. Based on our previous studies [14], the chemical energy per gram of energetic materials was 3.04 kJ. Taking the parameters of EPG-A equipment as an example, in the energy system of 3.0 kV/2.0 g, the energy deposited after the wire triggered the energetic materials was 1.07 kJ. Consequently, the energy released by the energetic materials accounted for 86% of the total energy system, indicating that the bulging height of the sheet was mainly contributed by the chemical energy released by energetic materials. From the perspective of the final bulging height, velocity variation trend and effective plastic strain value, the bulging results obtained under the two equipment parameters were basically consistent. Therefore, we conclude that the initial energy storage of the electric pulse generator can only provide triggering function for energetic materials, and the matching parameters of capacitance-voltage have no effect on the released energy level of energetic materials. In other words, energetic materials were insensitive to the initial equipment conditions of the electrical pulse generator, and had low requirements on the matching parameters of the capacitance-voltage of the equipment. The electric pulse generator can provide enough system triggering energy, which can trigger energetic materials to release energy stably, thus increasing the flexibility of initial equipment condition triggering. This will be beneficial to the popularization and application of ETEF. Subsequently, we select EPG-A equipment parameters to study the deformation of the sheet under ETEF in detail.

### 3.3. Analysis of deformation results of sheet metal

The bulging height, maximum strain value and maximum thinning rate of the bulged specimen during ETEF were used to analyze the deformation of DP600 sheet, as shown in Table 4. Fig. 6 shows the specimens and profiles obtained from ETEF and QSF tests with the same bulging height (24mm, 29mm). It can be seen that the non-uniform deformation of the QSF specimens occurred in the deformation zone 20–40 mm from the apex of the sheet. While the profile of the specimen under ETEF condition was more uniform. When the energetic materials was triggered by the metal wire to release energy, it would press the surrounding water medium to obtain kinetic energy and push the sheet to complete high-speed deformation. As a flexible “punch”, the water medium has certain fluidity, which improves the profile uniformity of the specimen. The thickness distribution is an important index to measure the deformation uniformity of deformed specimen. Fig. 7 shows the thickness distribution of the bulged specimens. In the deformation zone of φ100mm, the thickness distribution of the specimens under ETEF condition were relatively uniform, and the maximum thinning rate occurred in the apex area of the specimens, which was 15.3% (specimen NO.1) and 23.8% (specimen NO.2), respectively. Under the QSF condition, the thickness distribution of the specimens were deformed unevenly in the deformation zone, which resulted in a very serious thickness reduction, and the maximum values were 22.1% (specimen NO.3) and 27.6% (specimen NO.4), respectively. Therefore, compared with the quasi-static bulged specimens with the same bulging height (24mm, 29mm), the maximum thickness rate of the specimens under the conditions of ETEF/3.0kV/1.0g and ETEF/3.0kV/1.5g were reduced by 30.8% and 13.8%, respectively.

**Table 4** Summary of the ETEF and QSF test results.

| Specimen number | Type | Voltage (kV) | Energy(kJ) | EMs (g) | Dome height(mm) | Maximum strain (%) | | |
|---|---|---|---|---|---|---|---|---|
| | | | | | | Major strain | Minor strain | Thinning rate |
| **NO. 1** | ETEF | 3.0 | 1.368 | 1.0 | 24<br>29 | 9.24 | 8.16 | 15.3 |
| **NO. 2** | ETEF | 3.0 | 1.368 | 1.5 | 24<br>29 | 15.2 | 14.2 | 23.8 |
| **NO. 3** | QSF | - | - | - | | 16.7 | 12.1 | 22.1 |
| **NO. 4** | QSF | - | - | - | | 21.6 | 13.7 | 27.6 |

According to Table 4, the maximum major strain and the maximum thinning rate of the specimens obtained under ETEF were lower than those of QSF, which inevitably affected the strain distribution in the deformation zone of the specimens. Fig. 8 exhibits the strain distribution and thinning rate of ETEF/1.5g and QSF/29mm specimens with the same bulging height. The maximum major strain and the maximum minor strain of the specimen under the QSF condition were located 20mm from the apex of the sheet, and their values were 21.6% and 13.7%, respectively, and distributed symmetrically. Clearly, the maximum strain obtained by ETEF was distributed at the apex of the specimen, and its maximum major strain and maximum minor strain were 15.2% and 14.2%, respectively (Fig. 8(a)). In the deformation zone φ 60mm, the strain in two principal in-plane directions was almost equiaxial, therefore, the strain distribution was obviously improved, and the maximum major strain decreased by 29.6% compared with QSF. Moreover, the thinning rate also showed similar distribution characteristics, and the thinning rate of the specimen under ETEF conditions was significantly reduced compared with that of QSF (Fig. 8(b)). According to our previous tests [14], the specimen also cracked here under quasi-static conditions, mainly because the contact friction between the specimen and punch increased in the deformation zone, which resulted in a large deformation and serious thickness thinning in this zone

[22].Therefore, the maximum strain and thinning rate of ETEF specimens decreased, which significantly improved the uniformity of strain distribution in the deformation zone.

## 3.4. Dynamic deformation process of sheet metal

LS-DYNA simulation software was adopted to simulate the dynamic deformation process of the sheet in ETEF. A quarter geometric model (including: Mo wire, EMs, water, air, blank, blank holder and liquid chamber) was established based on the test tooling in Fig. 2(a). Then, the energy input in ETEF was preset, including the electrical energy input by metal wire (Fig. 3(c)) and the chemical energy of energetic materials. The former was the electric energy preset by the metal wire through the electric pulse generator, which mainly played the role of igniting energetic materials; the chemical energy of the latter was the energy released by the chemical reaction of energetic materials after being ignited by metal wire. The deformation of the sheet was mainly realized by the chemical energy released by energetic materials. The detailed implementation process of numerical simulation of ETEF can be consulted in our previous work [14].

According to the description in Section 2.2, energetic materials mainly produce heat energy, light energy and mechanical energy after releasing energy, and form shock waves to work on the surrounding water medium, resulting in plastic deformation of the workpiece. Therefore, the plastic strain energy was used to evaluate the contribution of energy released by energetic materials to the plastic deformation of the blank [23]. Fig. 9 shows the change with time of plastic strain energy of the blank after energy release by energetic materials in ETEF process. It can be found that the addition of energetic materials significantly increased the plastic strain energy of the blank. Compared with the final plastic strain energy of EHF/3kV, the plastic strain energy obtained under the conditions of ETEF/3kV/1.0g and ETEF/3kV/1.5g contributed 60% and 74% to the plastic deformation of the blank, respectively. Specifically, according to the research in Sections 3.1 and 3.2, it was found that the deposition energy consumed by energetic materials during ignition was about 200J, which was relatively small in the whole energy system and even negligible, but it reduced the deposition energy under EHF/3kV conditions. Therefore, the plastic strain energy obtained under the conditions of ETEF/3kV/1.0g and ETEF/3kV/1.5g contributed slightly more than 60% and 74% to the plastic deformation of the blank, respectively. As a result, the energy released by energetic materials in the ETEF process played a major role in the plastic deformation of the blank. Moreover, it can be seen from the changing trend of plastic strain energy of the blank that the increase of plastic strain energy can be divided into two stages. Taking ETEF/3kV/1.5g as an example, the plastic strain energy increased slightly within 60μs, and the plastic strain energy of the blank increased significantly in 60-300 μs. Therefore, after the energetic materials released energy, the shock wave pressure and the stress and strain on the blank must change significantly in different plastic deformation stages.

Figure 10 exhibits the change of the shock wave pressure generated by the elements on the metal wire and energetic materials with time during the ETEF process. Elements A, B, and C were on metal wire, and elements D, E, and F were on energetic materials. After the electric pulse generator discharged, the shock wave pressure of the elements on the metal wire and energetic materials were generated almost simultaneously, and the duration from the generation of the pressure to the rapid drop were about 10 μs. Remarkably, from the peak pressure on the elements, it can be found that the maximum value of the shock wave pressure generated by the elements on the energetic materials were greater than that on the metal wire, indicating that the energetic materials were ignited by the metal wire and increased the peak value of the shock wave. Therefore, according to the analysis in

Section 3.1, the addition of energetic materials increased the total energy of the system, that is, increased the pressure of shock wave, which is consistent with the conclusion of Zhou et al. [21]. After 10 μs, the pressure on the elements decreased slowly, only 8 MPa at 50 μs, and close to zero at 60 μs. Therefore, the total duration of the electrical energy of metal wire and the chemical energy generated by energetic materials was 60 μs.

Fig. 11 presents the result velocity and effective stress of the elements on the sheet over time. First, the metal wire and energetic materials released energy within 0-60 μs. At 24 μs, the shock wave pressure was transmitted to the sheet, which caused the effective stress on the sheet to increase rapidly, and the speed of the element L rapidly increased to the maximum value of 188 m/s. Next, due to the weakening of the initial electrical and chemical energy within 24-60 μs, the deformation speed of the sheet decreased. However, the effective stress on the sheet continued to increase, and the increase became slow at 50 μs, and then after 60 μs, the speed of the sheet increased again under the action of water flow pressure and inertia. Eventually, the effective stress decreased rapidly when it increased to 250 μs, and the deformation speed of the sheet also decreased rapidly at 200 μs, and the deformation ended at 300 μs. Therefore, the deformation process of sheet in ETEF can be divided into two stages: (i) the early stage of deformation (within 0-60 μs), and the initial chemical energy action stage of energetic materials; (ii) the late deformation period (within 60-300 μs) belongs to inertia action stage.

Fig. 12 shows the contours/vector of the bulging height (Y-displacement) of the tested specimen during the ETEF process. In the initial chemical energy action stage of energetic materials, the bulging height of the specimen at 60 μs was only 7.5mm, presenting a conical bulging profile, as shown in Fig. 12(a). At 120 μs, the specimen showed an approximately ellipsoidal bulging profile (Fig. 12(b)), and the deformation profile was further improved. At 200 and 300 μs, the profile of the bulged specimen was hemispherical, and the bulging height of the final specimen is 30.1mm, with an error of only 3.8% from the experimental bulging height of 29mm (Table 4). Therefore, in the inertia action stage (within 60-300 μs), the bulging height of the specimen increased by 301% compared with the initial chemical energy action stage of the energetic materials. The inertia effect accounted for 80% of the total deformation time, which significantly increased the bulging height of the sheet metal and played a leading role in the plastic deformation.

The profile change of the bulging specimen during the ETEF process will inevitably affect the distribution of the effective plastic strain. The variation of the effective plastic strain of the deformed specimen at different times is shown in Fig. 13. At 30 μs, the effective plastic strain with elliptical annular distribution appeared on the specimen; At 60 μs, the effective plastic strain presented a rectangular distribution in the central deformation zone of the specimen, at this time, the width of the strain concentration zone was parallel and equal to the geometric dimension of EMs cylinber (Fig. 2(a)). At 100 μs, the effective plastic strain concentration area was elliptical (the ratio of long axis to short axis: 1.6), and the strain distribution was extremely uneven. At 120 μs, the effective plastic strain in the central deformation zone was close to a circle (the ratio of long axis to short axis: 1.1), and the effective plastic strain was significantly improved. Within 200-300 μs, the effective plastic strain in the central deformation zone was uniformly distributed. These results further indicate that the energy released by energetic materials during the ETEF process can significantly improve the distribution of effective plastic strain, which is of great significance for forming axisymmetric parts.

# 4. Conclusions

In this research, the technological characteristics of ETEF were revealed from the aspects of pulse discharge characteristics and dynamic deformation process of sheet metal. To achieve this goal, experiments and numerical simulations were carried out. The conclusions of this study can be summarized as follows:

1. In the process of triggering energetic materials by electric pulse, due to the addition of energetic materials, the waveform amplitude of discharge voltage and current decreased, and the peak value of current decreased significantly. Additionally, the electric power and deposition energy generated by discharge of different pulse equipment also decreased, and the triggering energy consumption of energetic materials was quantified to be about 200J.
2. The matching parameters of different capacitor-voltage equipment had no effect on the energy release of energetic materials, which showed that the maximum deformation speed, bulging height and effective plastic strain of the sheets after energy release of energetic materials were at similar levels. Therefore, with sufficient system energy storage, the electric pulse equipment only triggered the energetic materials, and did not affect the energy release.
3. Compared with the quasi-static specimen with the same bulging height (29mm), the maximum major strain and the maximum thinning rate of the bulged specimen under ETEF/3kV/1.5g decreased by 29.6% and 13.8%, respectively, which significantly improved the strain distribution, thickness distribution and deformation uniformity of the sheet.
4. The simulation results showed that the addition of energetic materials significantly improved the plastic strain energy of the blank. Compared with EHF/3kV, the final plastic strain energy obtained under the conditions of ETEF/3kV/1.0g and ETEF/3kV/1.5g contributed 60% and 74% to the plastic deformation of the blank, respectively.
5. (i) In the initial chemical energy action stage of energetic materials, the effective stress on the blank increased rapidly, and the maximum speed reached 188 m/s. (ii) In the inertia action stage, the bulging height of the specimen increased by nearly 301%, and the error between the final bulging height and the experiment was only 3.8%. During ETEF, the effective plastic strain of sheet metal was significantly improved, and inertia effect accounted for 80% of the total deformation time, which played a leading role in plastic deformation.

# Declarations

Funding

This work was supported by the National Natural Science Foundation of China [Grant No. 52175304]. The authors would like to take this opportunity to express their sincere appreciation.

Conflict of interest

The authors declare that they have no conflict of interest.

Availability of data and materials

All data generated or analysed during this study are included in this manuscript.

Code availability

Not applicable.

Ethical approval

Not applicable.

Consent to participate

Not applicable.

Consent to publish

Not applicable.

Authors' contributions

Xueyun Xie: Investigation, Writing-original draft, Writing-review & editing, Validation.

Haiping Yu: Writing-review & editing, Investigation, Supervision, Funding acquisition.

Yang Zhong: Reviewed and improved the manuscript.

# References


1. Daehn GS (2006) High-velocity metal forming. Metal working: Sheet Forming (ASM Handbook) vol.14. p.405–418
2. Ponnusamy P, Masood S H, Ruan D, Palanisamy S, Rashid R (2018) High strain rate dynamic behaviour of AlSi12 alloy processed by selective laser melting. Int J Adv Manuf Technol
3. Zheng QL, Yu HP, Cai, XH (2020) Formability and deformation behavior of DP600 steel sheets during a hybrid quasi-static/dynamic forming process. Int J Adv Manuf Technol 110(7-8):1-12
4. Sorgente D,  Palumbo G, Scintilla LD, Tricarico, L (2016) Gas forming of an AZ31 magnesium alloy at elevated strain rates. Int J Adv Manuf Technol 83(5-8):861-872
5. Psyk V, Risch D, Kinsey BL, Tekkaya AE, Kleiner M (2011) Electromagnetic forming—a review. J Mater Process Technol 211:896–908
6. Wang L, Chen ZY, Li CX, Huang SY (2006) Numerical simulation of the electromagnetic sheet metal bulging process. Int J Adv Manuf Technol 30(5-6):395-400
7. Noh HG, Song WJ, Kang BS, Kim J (2015) Two-step electromagnetic forming process using spiral forming coils to deform sheet metal in a middle-block die. Int J Adv Manuf Technol 76(9-12):1691-1703
8. Imbert J, Winkler S, Worswick M, Oliveira D, Golovashchenko S (2005) The effect of tool–sheet interaction on damage evolution in electromagnetic forming of aluminum alloy sheet. J Eng Mater Technol 127 (1):145–153
9. Dehra MS (2006) High velocity formability and factors affecting it. The Ohio State University 1-301
10. Golovashchenko SF, Gillard AJ, Mamutov AV, Bonnen JF, Tang JZ (2014) Electrohydraulic trimming of advanced and ultra high strength steels. J Mater Process Technol 214 (4):1027–1043

11. Tang JZ, Golovashchenko SF, Bonnen JF, Mamutov AV, Gillard AJ, Bonnen D (2014) Analysis of loads on the shearing edge during electrohydraulic trimming of AHSS steel in comparison with conventional trimming. J Mater Process Technol 214(12):2843-2857
12. Mamutov AV, Golovashchenko SF, Mamutov VS, Bonnen JJF (2015) Modeling of electrohydraulic forming of sheet metal parts. J Mater Process Technol 219:84–100
13. Efimov S, Gurovich VT, Bazalitski G, Fedotov A, Krasik YE (2009) Addressing the efficiency of the energy transfer to the water flow by underwater electrical wire explosion. J Appl Phys 106(7):2282
14. Yu HP, Xie XY, Zheng QL (2021) A novel method of processing sheet metals: electric-pulse triggered energetic materials forming. J Mater Process Technol
15. Han RY, Zhou HB, Wu JW, Qiu AC, Ding WD, Zhang YM (2017) Relationship between energy deposition and shock wave phenomenon in an underwater electrical wire explosion. Phys Plasmas 24(9):093506
16. Grinenko A, Sayapin A, Gurovich VT, Efimov S, Felsteiner J, Krasik YE (2005) Underwater electrical explosion of a cu wire. J Appl Phys 97(2):1165
17. Timoshkin IV, Fouracre RA, Given MJ, Macgregor SJ (2006) Hydrodynamic modelling of transient cavities in fluids generated by high voltage spark discharges. J Phys D Appl Phys 39:1-10
18. Pagoria PF, Lee GS, Mitchell AR, Schmidt RD (2002) A review of energetic materials synthesis. Thermochim Acta 384(1):187-204
19. Cai Y, Zhao FP, An Q, Wu H, Luo SN (2013) Shock response of single crystal and nanocrystalline pentaerythritol tetranitrate: implications to hotspot formation in energetic materials. J Chem Phys 139(16):164704
20. Han RY, Zhou HB, Liu QJ, Wu JW, Yan J, Chao YC, Zhang YM, Qiu AC (2015) Generation of electrohydraulic shock waves by plasma-ignited energetic materials: I. Fundamental mechanisms and processes. IEEE T Plasma Sci 43 (12):3999–4008
21. Zhou HB, Han RY, Liu QJ, Yan J, Wu JW, Zhang YM, Qiu AC, Zhao YZ (2015) Generation of electrohydraulic shock waves by plasma-ignited energetic materials: II. Influence of wire configuration and stored energy. IEEE T Plasma Sci 43(12):4009-4016
22. Li C, Chi CZ, Lin P, Zhang H, Liang W (2015) Deformation behavior and interface microstructure evolution of Al/Mg/Al multilayer composite sheets during deep drawing. Mater Des 77:15-24
23. Shi J, Cao X, Shen C (2015) Damage criteria based on plastic strain energy intensity under complicated stress state. Int J Appl Mech 07(06):1550089

# Figures

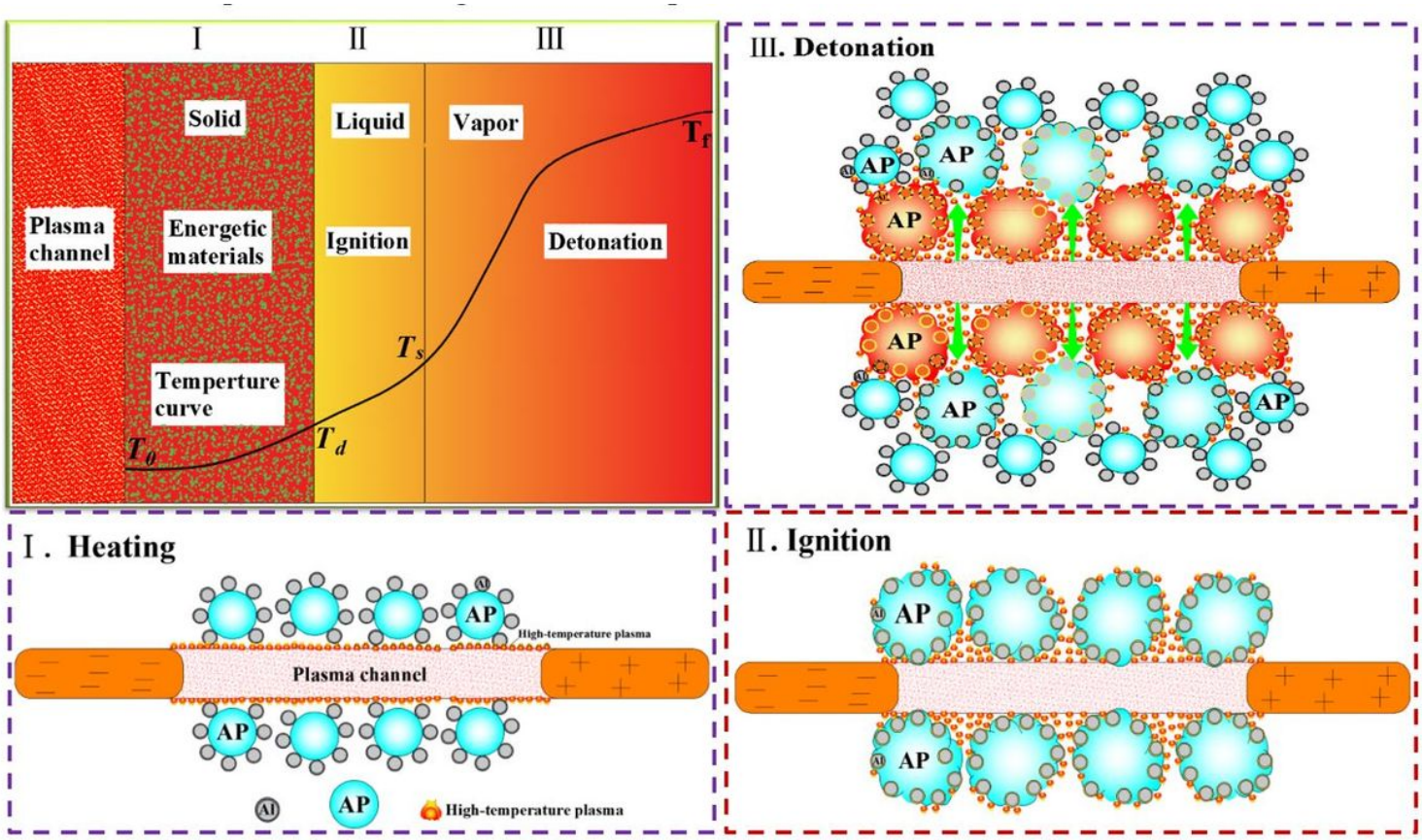


## Figure 1

Schematic diagram of energetic materials ignited by plasma.

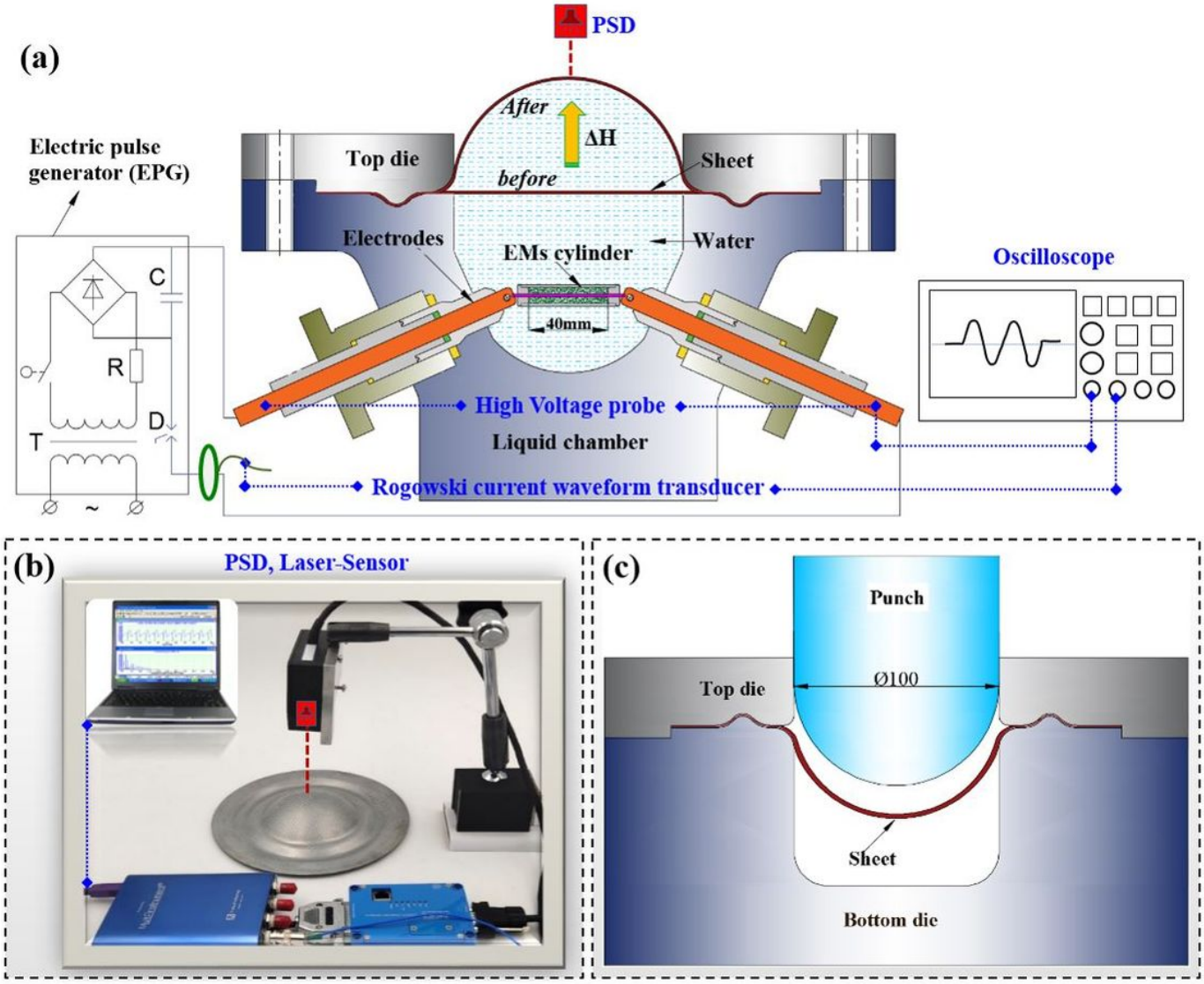


## Figure 2

Schematic of experimental setup under free bulging tests: (a) ETEF, (b) Laser-Sensor M70LL and (c) Quasi-static free bulging.

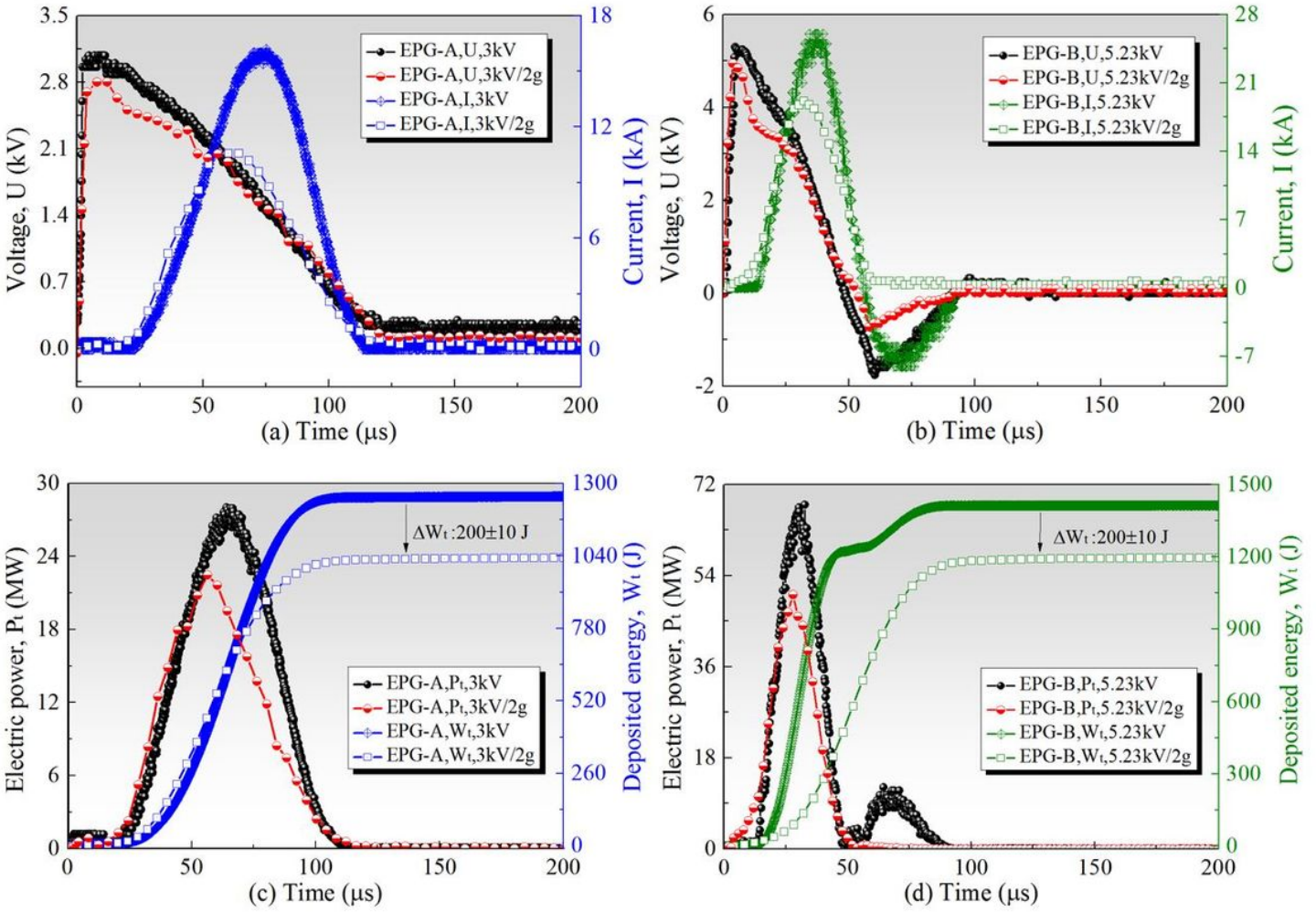


**Figure 3**

Electrical parameter waveforms: (a) current and voltage waveforms of EPG-A, (b) current and voltage waveforms of EPG-B, (c) electric power and deposited energy waveforms of EPG-A and (d) electric power and deposited energy waveforms of EPG-B.

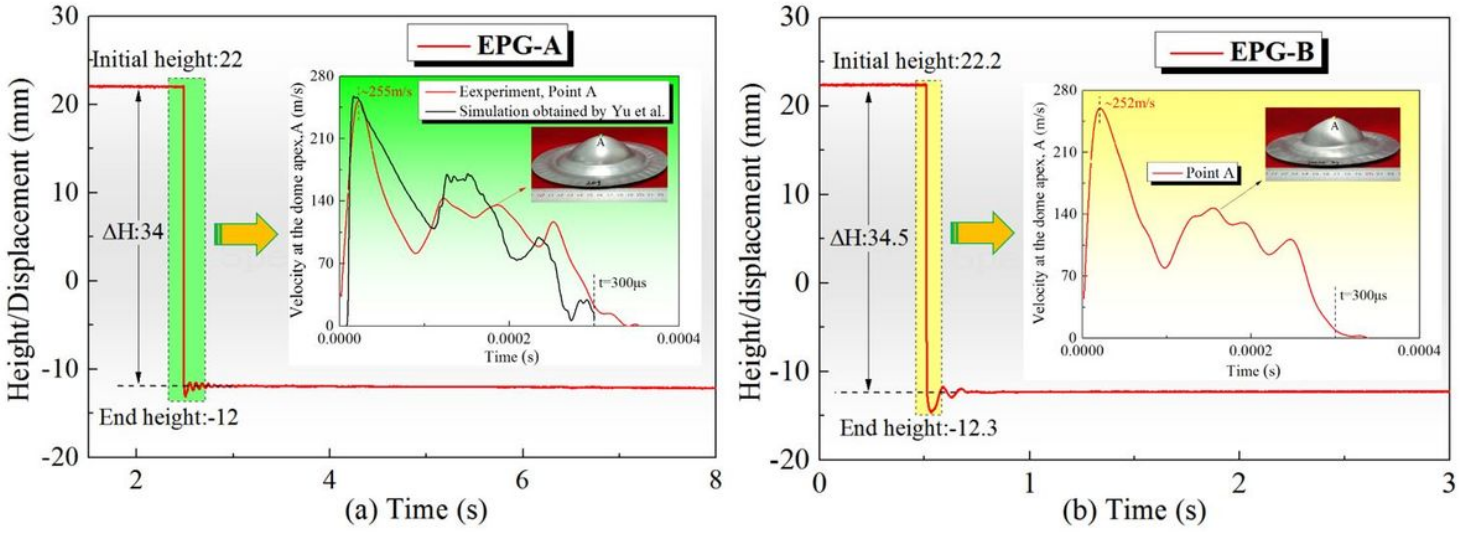


**Figure 4**

The variation of apex displacement and velocity of bulging specimen with time under different equipment parameters (a) EPG-A and (b)

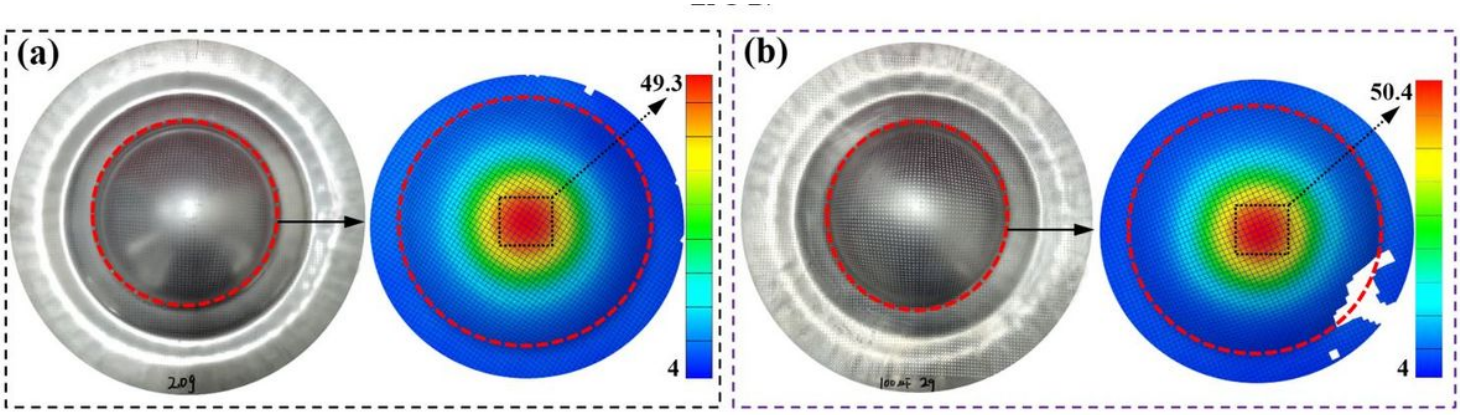


**Figure 5**

The effective plastic strain distribution of bulging specimen under different equipment parameters (a) EPG-A and (b) EPG-B.

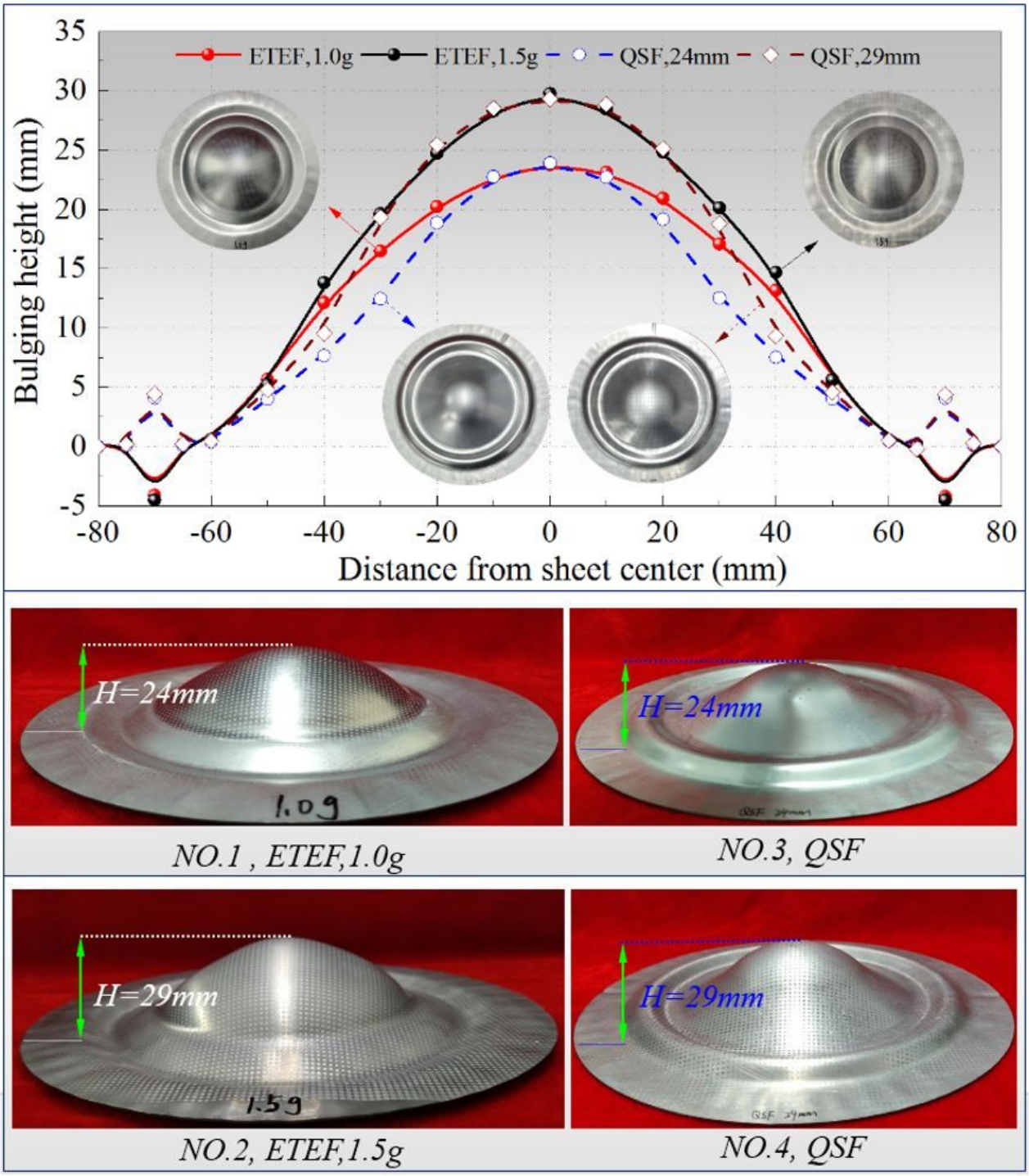


**Figure 6**

The specimens and profiles obtained from ETEF and QSF tests with the same bulging height (24mm, 29mm).

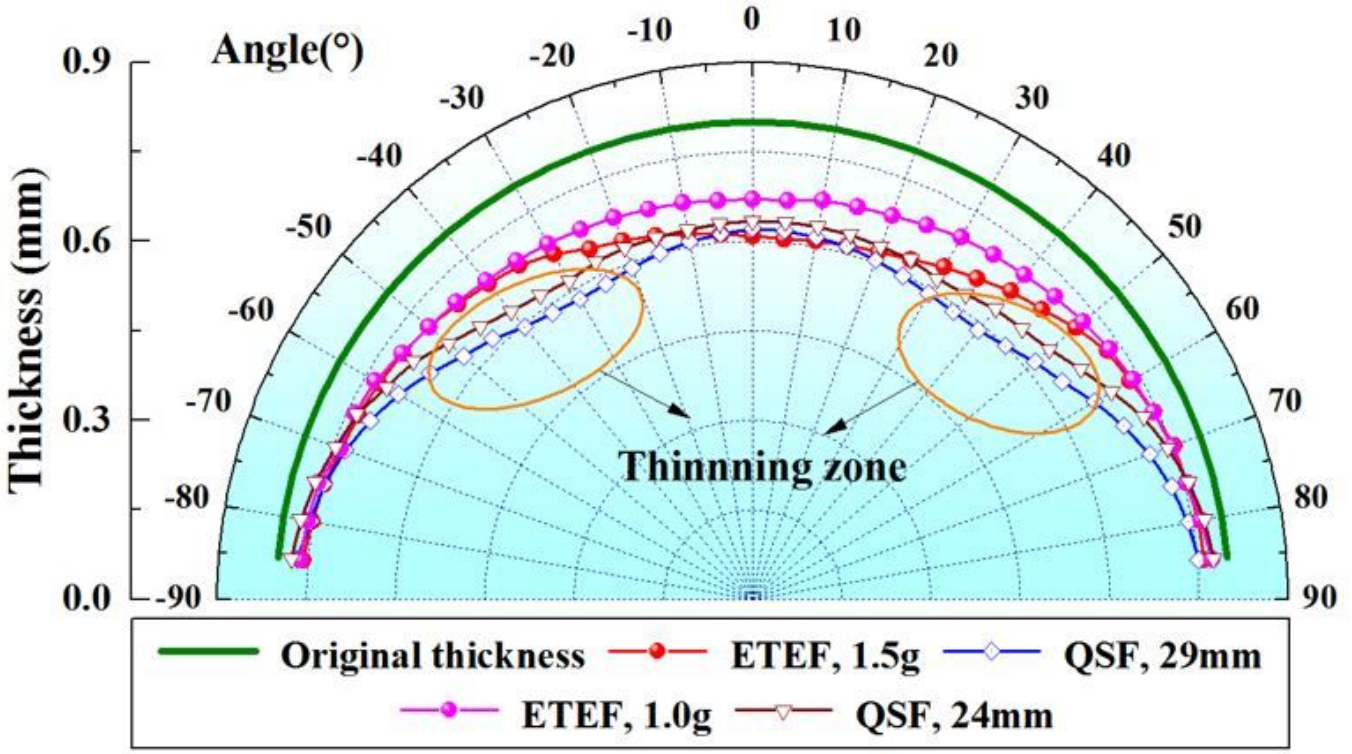


## Figure 7

The thickness distribution of the bulged specimens.

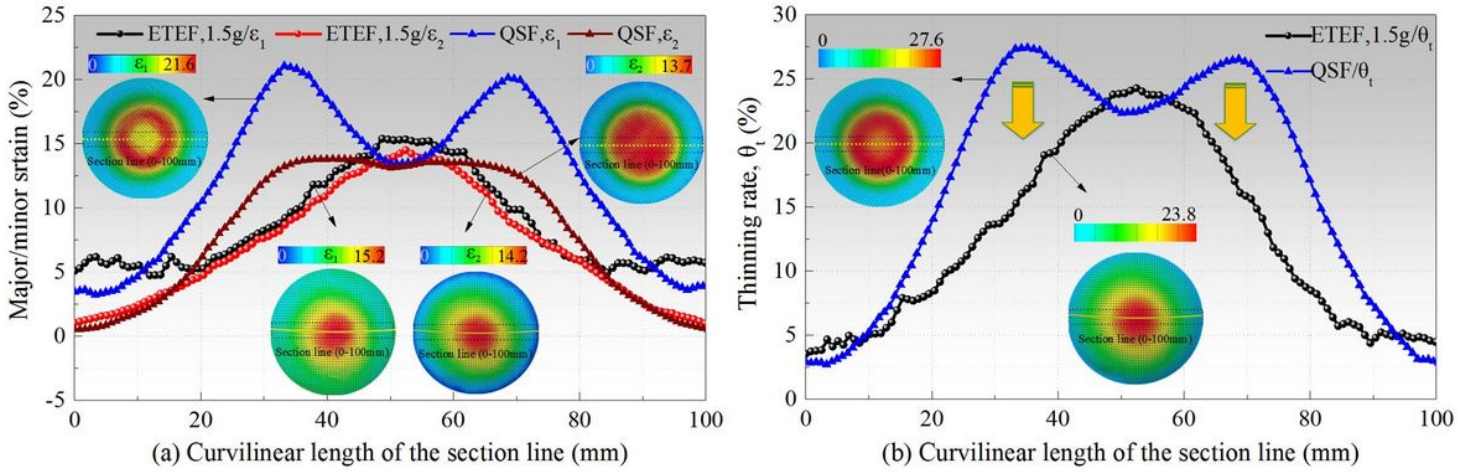


## Figure 8

(a) Strain distribution and (b) thinning rate obtained by bulged specimens under ETEF and QSF conditions.

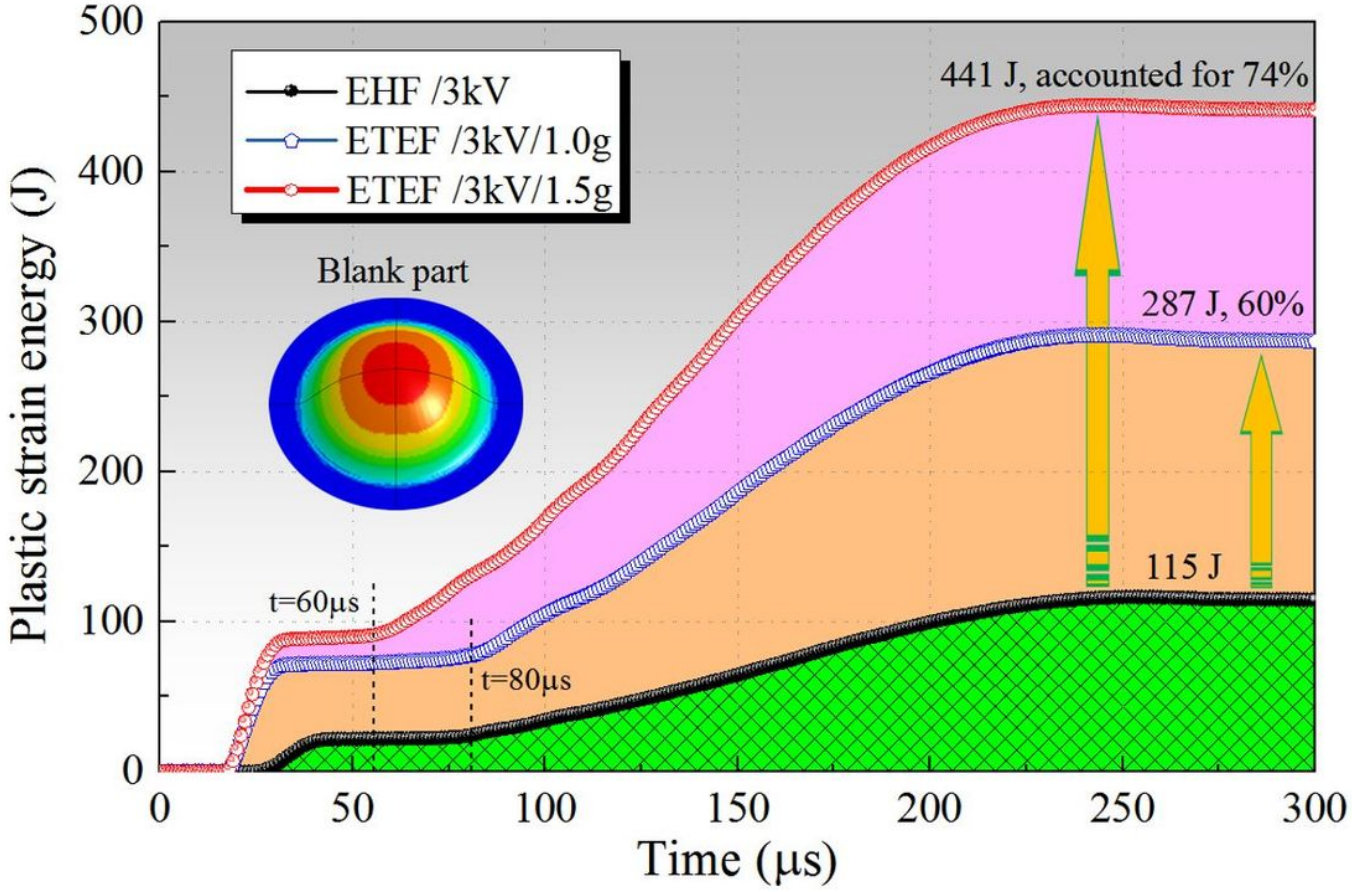


**Figure 9**

Variation of plastic strain energy of the bulged specimen with time in ETEF process.

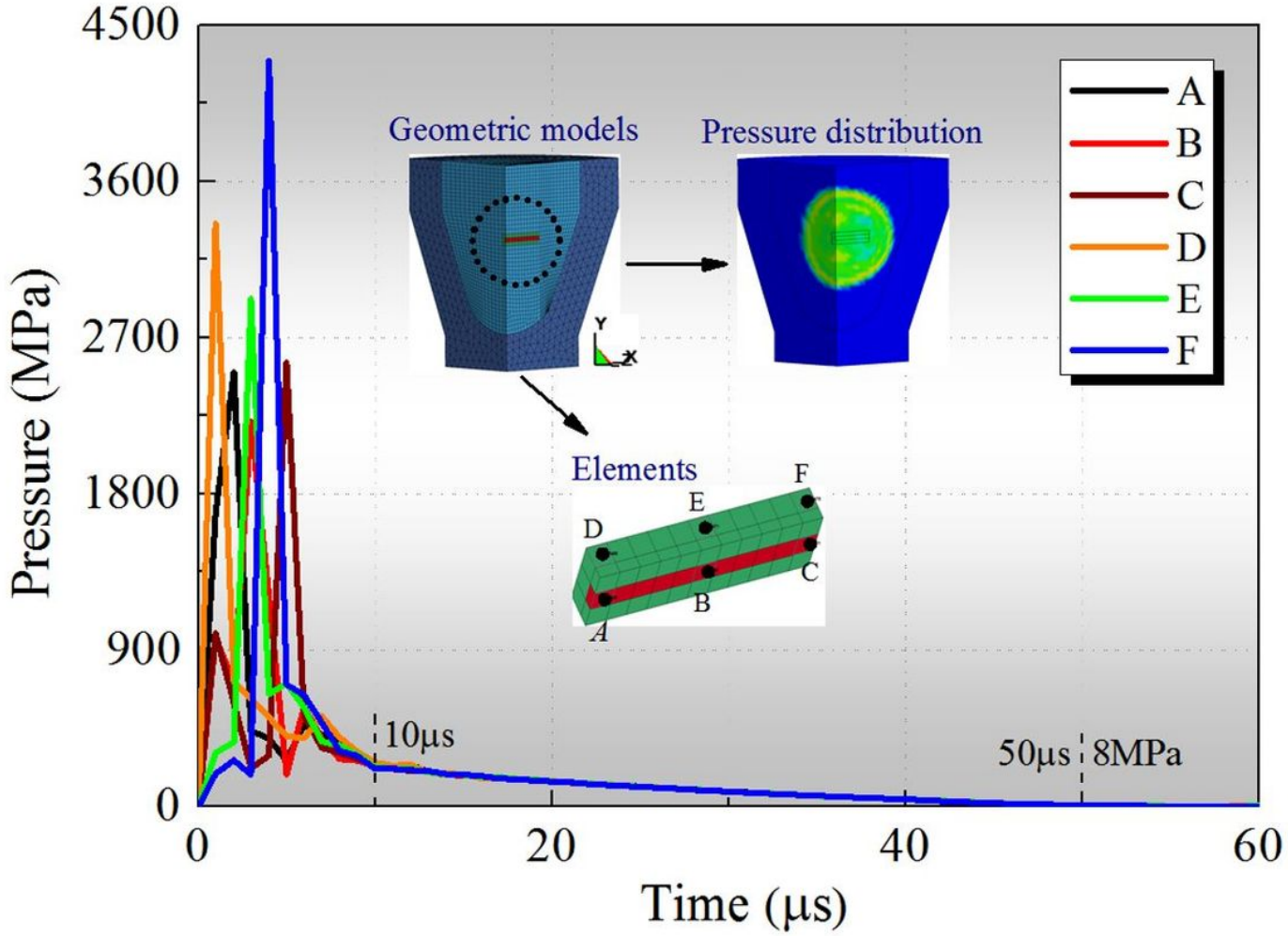


**Figure 10**

The curves of the elements shock wave pressure on metal wire and energetic materials.

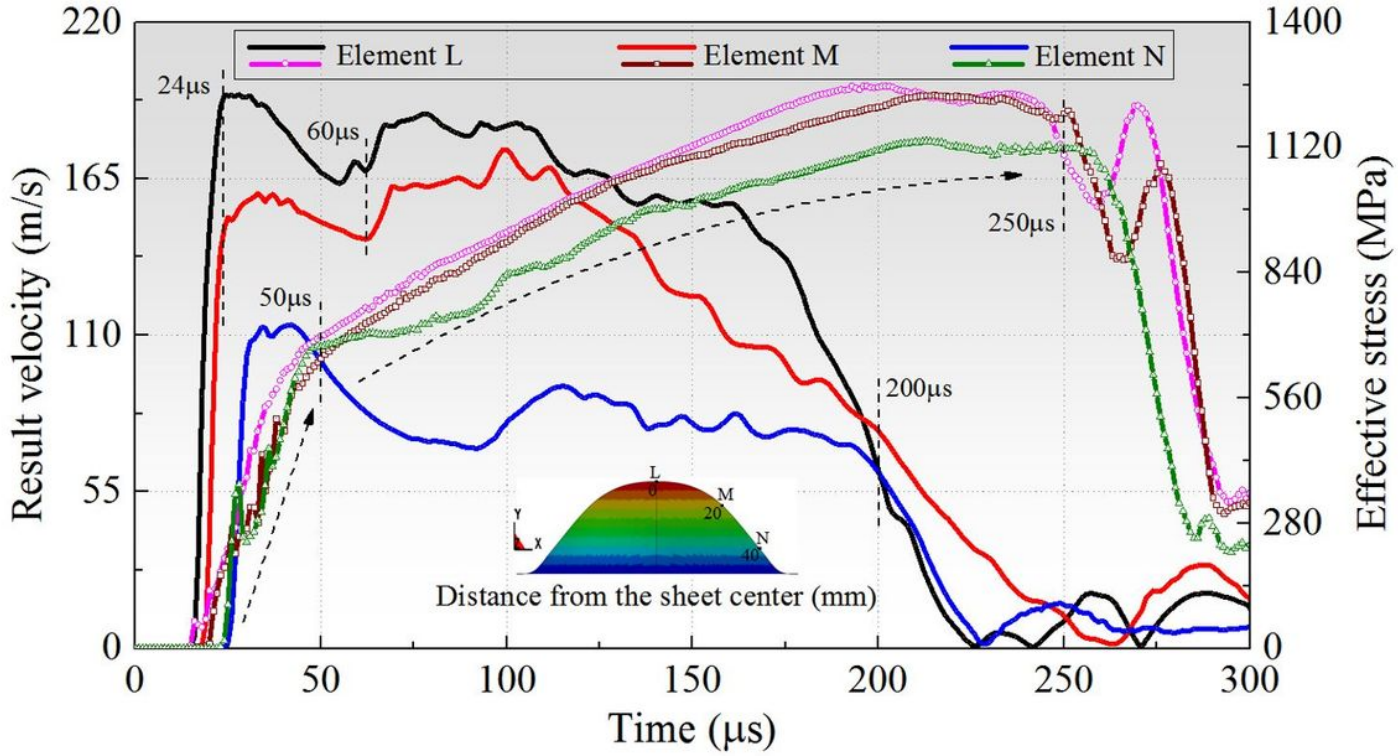


**Figure 11**

Result velocity/effective stress versus time of the selected elements during the ETEF process.

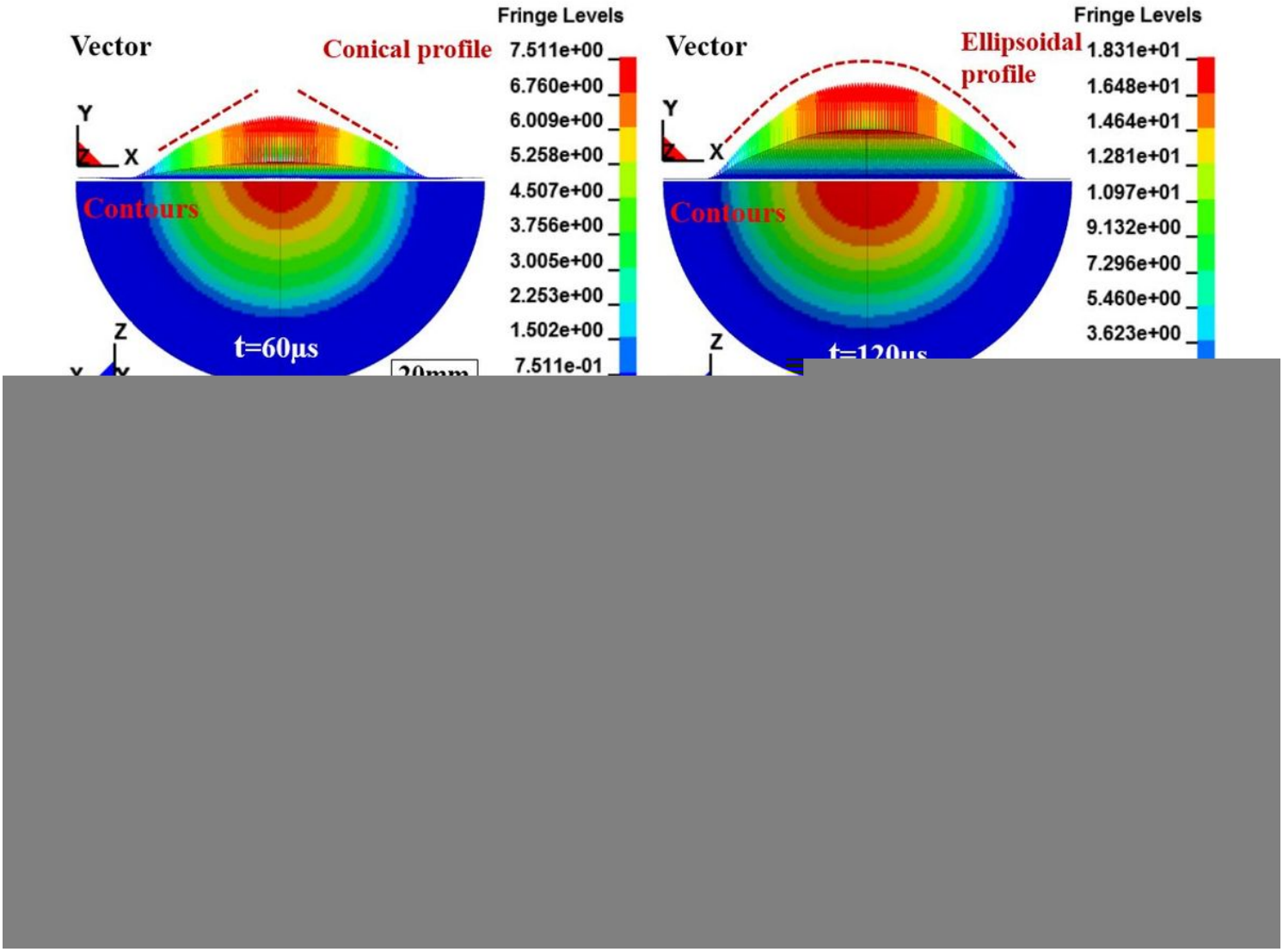


Figure 12

The contours/vector of Y-displacement of the tested specimen.

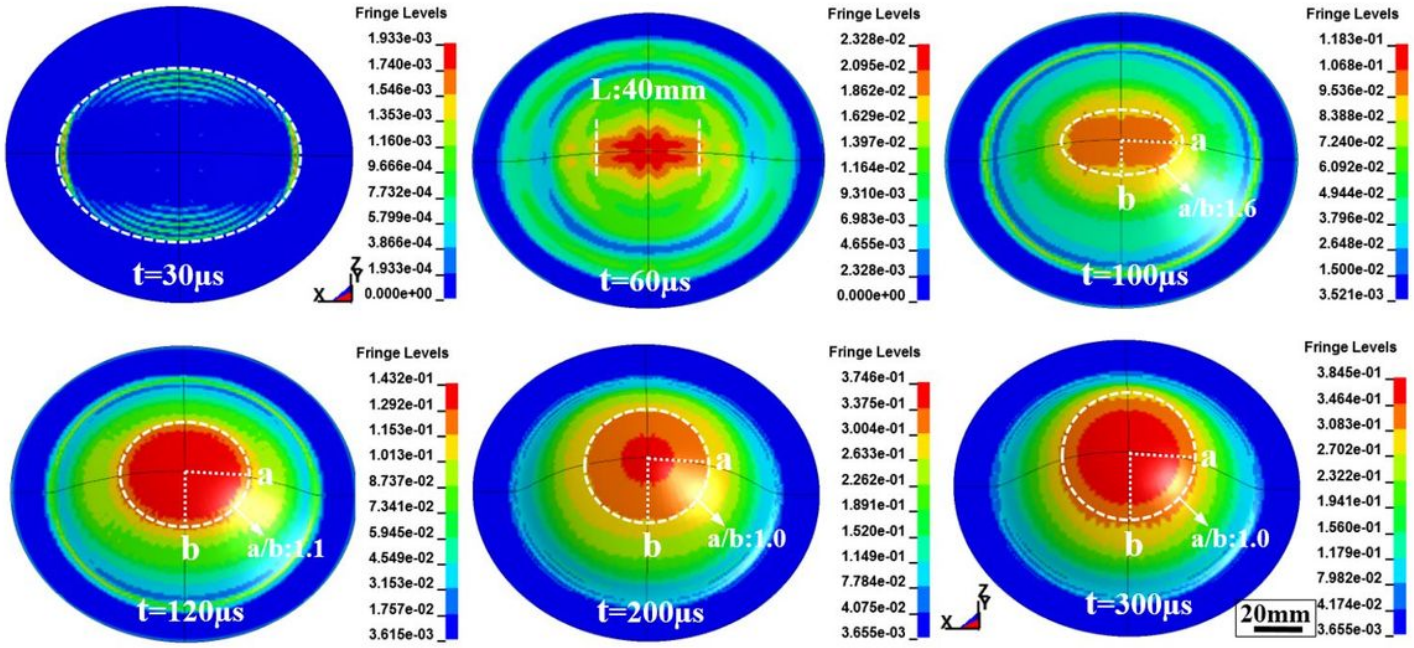


## Figure 13

The contours of the effective plastic strain of the tested specimen during the ETEF process.